Title	Majorana fermions qubit states and non-Abelian braiding statistics in quenched inhomogeneous spin ladders
Author(s)	He, Y; Chen, Y
Citation	Physical Review B (Condensed Matter and Materials Physics), 2013, v. 88 n. 18, p. article no. 180402
Issued Date	2013
URL	http://hdl.handle.net/10722/193894
Rights	Creative Commons: Attribution 3.0 Hong Kong License

PHYSICAL REVIEW B **88**, 180402(R) (2013)

Majorana fermions qubit states and non-Abelian braiding statistics in quenched inhomogeneous spin ladders

Yin-Chen He[1] and Yan Chen[1,2]

[1]*Department of Physics, State Key Laboratory of Surface Physics and Laboratory of Advanced Materials, Fudan University, Shanghai 200433, China*

[2]*Department of Physics and Center of Theoretical and Computational Physics, The University of Hong Kong, Pokfulam Road, Hong Kong, China*

(Received 11 February 2013; revised manuscript received 30 October 2013; published 18 November 2013)

In studying Majorana fermions (MFs) in a spin ladder model, we numerically show that their qubit state can be read out by measuring fusion excitations in quenched inhomogeneous spin ladders. We construct an exactly solvable T-junction spin ladder model that can be used to implement MF braid operations. With braiding simulated numerically as nonequilibrium quench processes, we verify that the MFs in our spin ladder model obey non-Abelian braiding statistics. Our scheme provides a promising platform to study exotic properties of MFs and a broad range of applications in topological quantum computation.

DOI: 10.1103/PhysRevB.88.180402 PACS number(s): 03.65.Vf, 03.67.Lx, 05.30.Pr, 75.10.Jm

Majorana fermions (MFs) are self-conjugate quasiparticles ($\gamma^\dagger = \gamma$),[1] and non-Abelian anyons obeying exotic braiding statistics.[2,3] Recent years have seen much excitement over MFs, not only because of their peculiar properties, but also due to the possible applications for topological quantum computation.[4] Creating, manipulating, and detecting MFs experimentally remains a great challenge, although many schemes for doing that have been proposed.[5–21] As far as their realization is concerned, encouraging progress has been made for one-dimensional (1D) systems, especially for semiconducting wires,[22] where a zero-bias conductance peak (ZBCP)[23] and a fractional Josephson effect[24] have been recently measured. However, controversy remains about whether those experimental signatures indicate the realization of MFs.[25,26] Moreover, to our knowledge, so far there exists no unambiguous and straightforward evidence to demonstrate the braiding statistics of MFs.

Although the superconducting (SC) system is a natural choice to create MFs, spin systems have received considerable attention since the pioneering work of Kitaev.[27] Creating MFs in 1D spin systems is quite different from their creation in electronic systems. For instance, superconductivity cannot emerge spontaneously in a semiconductor wire; instead it is induced by proximity to a superconductor. This fact imposes extra difficulty in creating and controlling MFs in such systems. In contrast, one only needs to engineer the desired spin-spin interaction in the spin system. Since spin systems are produced in highly controllable quantum simulations,[28–33] the latter could provide promising platforms for creating and controlling MFs in actual experiments.

Despite recent extensive theoretical studies of MFs in 1D spin systems,[34–37] the applicability of non-Abelian braiding statistics to MFs in such systems remains unclear, as is a clear method to implement the braid operations. In this Rapid Communication, we propose and numerically confirm that one can read out the MF's qubit state by measuring the resulting fusion excitation in a spin ladder system, while suppressing undesired excitations by inhomogeneity. Moreover, we design an exactly solvable T-junction spin ladder model which can be used to implement the braid operation. By numerically simulating this operation as a nonequilibrium process, we verify that the MFs obey non-Abelian braiding statistics, thus providing a platform for the experimental realization of topological quantum computation.

The Hamiltonian and its features. The Hamiltonian of a single spin ladder[36,37] can be written as

$$H = -\sum_{\langle i,j\rangle} J_{ij}^{\beta_{ij}} \sigma_i^{\beta_{ij}} \sigma_j^{\beta_{ij}}, \quad \beta_{ij} = x,y,z, \tag{1}$$

where $\sigma^{x(y,z)}$ are the Pauli operators. We have decomposed the links of the spin ladders into three classes, as exemplified in Fig. 1; each link class is associated with one component of the interaction $J^\tau \sigma_i^\tau \sigma_j^\tau$, $\tau = x,y,z$.

To solve the Hamiltonian equation (1), we represent each spin operator as the product of two MF operators:[27,37]

$$\sigma_n^x = i b_n^x c_n, \qquad \sigma_n^y = i b_n^y c_n, \qquad \sigma_n^z = i b_n^z c_n, \tag{2}$$

where all the MF operators $b_n^{x,y,z}$ and c_n satisfy self-adjoint and anticommutation relations. Using the MF representation, the Hamiltonian takes the form

$$H = \sum_{\langle i,j\rangle} J_{ij}^{\beta_{ij}} \left(i b_i^{\beta_{ij}} b_j^{\beta_{ij}}\right)(i c_i c_j). \tag{3}$$

Note that the relation $\sigma_x\sigma_y\sigma_z = i$ imposes a constraint on the product of all MF operators $D_i = b_i^x b_i^y b_i^z c_i = 1$. Therefore, after obtaining the eigenstate $|\psi\rangle$ of the fermionic Hamiltonian, Eq. (3), one projects it into physical Hilbert space:

$$|\psi\rangle_{\text{phy}} = \hat{P}|\psi\rangle = \left(\prod \frac{1+D_i}{2}\right)|\psi\rangle. \tag{4}$$

In the spin ladder, each site has three links with different interaction terms. Therefore, $u_{ij} = i b_i^{\beta_{ij}} b_j^{\beta_{ij}}$ commutes with Eq. (3), taking the value ± 1 and, as a result, we obtain an exactly solvable quadratic Hamiltonian. Introducing for convenience the fermionic operator $f_n = (c_{2n-1} + i c_{2n})/2$, the

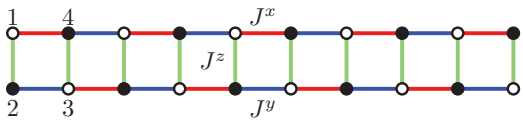

FIG. 1. (Color online) Spin ladders with three link classes.

Hamiltonian is expressible as

$$H = \sum_{n=1}^{N-1}[(\omega_n f_n^\dagger f_{n+1} + \Delta_n f_n f_{n+1} + \text{H.c.}) + \mu_n(2 f_n^\dagger f_n - 1)], \tag{5}$$

where $\omega_n = J_n^x u_{2n-1,2n+2} - J_n^y u_{2n,2n+1}$, $\Delta_n = J_n^x u_{2n-1,2n+2} + J_n^y u_{2n,2n+1}$, $\mu_n = J_n^z u_{2n-1,2n}$. This fermionic Hamiltonian equation (5) describes Kitaev's SC wire for the p wave.[11] For simplicity, we assume that the intrachain coupling J_n^x, J_n^y is positive and homogeneous. Then, one can verify that if $|J_n^z| < |J^x - J^y|$ the ground state corresponds to all $u_{ij} = 1$ $(i < j)$;[37] such chains are in a topological phase with two MFs located at the ends of the chain.

Detecting MFs qubit states. Two MFs can fuse into either a vacuum $|0\rangle$ or one fermion state $|1\rangle$, which can be treated as a qubit state.[4] Measuring the qubit state of the two MFs is important in processes executing topological quantum computations as well as in experimental realizations of MFs. Because MFs are zero energy modes in the topological phase, both qubit states $|0\rangle$ and $|1\rangle$ are ground states of the system that are hard to distinguish. In electronic systems, an anyon interference device like a Fabry-Perot interferometer has been designed to detect MF qubit states.[7,8] As far as our system is concerned, a similar interference device has not yet been developed.

Here, we propose a straightforward scheme to realize a MF qubit readout, where one directly fuses the MFs adiabatically and measures the emergent excitation. The so-called fusing of MFs, simply drives the system across the quantum critical point (QCP), from a topological phase to a nontopological phase. These two MFs in the qubit state $|1\rangle$ will then fuse into an excitation, making it easier to detect. In particular, in the spin system, the MF fusion excitation behaves like a spin flip that can be easily detected in highly controllable quantum simulations. However, the likelihood is that the described process might not be adiabatic due to the vanishing energy gap and divergent relaxation time at the QCP. These factors inevitably lead to the creation of many excitations, whose number is determined by the Kibble-Zurek mechanism (KZM).[38,39] The KZM excitations obscure detection of the MFs fusion excitations and therefore the suppression of these KZM excitations is necessary. In the following, we introduce inhomogeneity to realize this suppression of the KZM excitations.[40] This physical result can be understood qualitatively as follows: When an inhomogeneous system undergoes quenching, the critical point will be crossed locally and the whole energy spectrum always has a finite gap during quenching. Moreover, MFs can be located at the natural topological trivial and nontrivial interface resulting from an inhomogeneous potential, and move together at the critical point during quenching, thereby providing a means to manipulate the MFs.

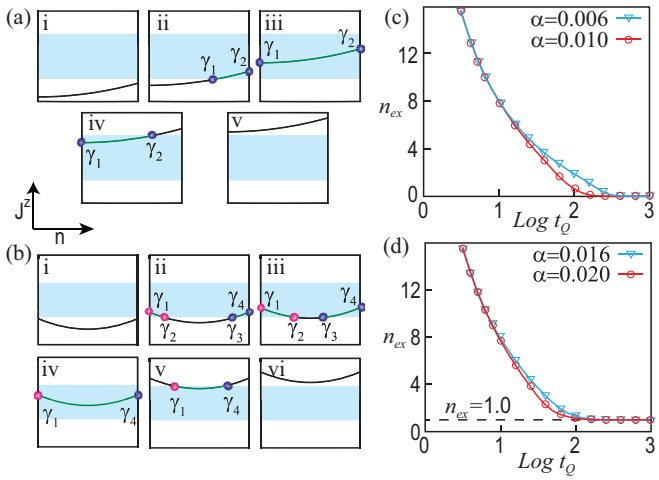

FIG. 2. (Color online) Diagrams for the two quench processes I (a) and II (b). Topological phase regions are marked in light cyan. MFs with the same color, (γ_1,γ_2) and (γ_3,γ_4), are paired MFs, which will fuse into the vacuum state $|0\rangle$. The number of excitations after the quench processes I (c) and II (d). Here we choose $J^x = 1.1$, $J^y = 0.1$.

Numerical simulations. To confirm that one can measure the MF qubit state by detecting the emergent excitations after a quench, we consider two simple processes, both of which have MFs created and fused. During a ramp, the interchain coupling J^z is inhomogeneous and varies with time:

$$\begin{aligned} &\text{Process I:} \quad J_n^z(t) = \alpha^2 n^2 + J_0 + t/t_Q, \\ &\text{Process II:} \quad J_n^z(t) = \alpha^2 (n - N/2 - 1/2)^2 + J_0 + t/t_Q, \end{aligned} \tag{6}$$

where α denotes the coefficient of a parabolic inhomogeneity. In the following, we choose the system size $N = 100$. With an increase of α, the minimum gap during the entire adiabatic quenching also increases, making it easier to suppress the KZM excitations. The term t/t_Q in Eq. (6) represents the quench with quench time t_Q, which determines the rate of change in the coupling strength. During the two quenches, the coupling strength will be ramped from $J_n^z < -|J^x - J^y|$ to $J_n^z > |J^x - J^y|$.

These two processes are shown schematically in Figs. 2(a) and 2(b). In quench process I, we create two paired MFs from the vacuum [Fig. 2(a), i and ii]. Without the participation of other MFs, these two MFs are always in the state $|0\rangle$. Thus, as one fuses the two MFs [Fig. 2(a), iv and v] to read out the qubit state, no excitations emerge. Quench process II has four MFs (γ_1,γ_2) and (γ_3,γ_4) drawn from the vacuum [Fig. 2(b), i and ii] for which the qubit state can be written as $|0,0\rangle$ in the basis $f_A = \gamma_1 + i\gamma_2$ and $f_B = \gamma_3 + i\gamma_4$. Interestingly, the two unpaired MFs, γ_2 and γ_3, will fuse at potential center, as depicted in Fig. 2(b), iii and iv. Therefore, this process actually measures the MF qubit state in the basis $f_A' = \gamma_2 + i\gamma_3$, $f_B' = \gamma_1 + i\gamma_4$. Written in the f_A', f_B' basis, $|0,0\rangle$ is $(|0'0'\rangle - i|1'1'\rangle)/\sqrt{2}$, which implies the emergence of one excitation. Clearly, this readout scheme is insensitive to the relative phase factor between $|0'0'\rangle$ and $|1'1'\rangle$. However, this relative phase can be read out by fusing the MFs in other pairs, such as (γ_1,γ_2) and (γ_3,γ_4). Generally speaking, if one measures a state $(|0'0'\rangle + ie^{i\theta}|1'1'\rangle)/\sqrt{2}$, in the basis

$f_A = \gamma_1 + i\gamma_2$, $f_B = \gamma_3 + i\gamma_4$, the fusion excitation with number $n = 1 + \cos\theta$ emerges.

To verify the above scenario, we performed numerical simulations of the dynamics for the two quench processes. Using the Bogoliubov transformation $a_m^\dagger = \sum_n (u_{nm} f_n^\dagger + v_{nm} f_n)$, we can diagonalize the Hamiltonian at any given time, and find that for both quench processes there is always an energy gap.[41] We consider an initial BCS ground state of the ladder $|\psi\rangle = \hat{P}\prod a_i^\dagger|0\rangle/N_0$, and a final state is $|\psi_f\rangle = \hat{P}\prod a_i^\dagger(t_f)|0\rangle/N_0$ with

$$\hat{a}_m^\dagger(t_f) = U\hat{a}_m^\dagger U^\dagger, \quad U = T\left\{\exp\left[-i\int_{t_0}^{t_f} H(t)dt\right]\right\}, \quad (7)$$

where N_0 is a normalization constant, $U(t)$ is a time evolution operator, and T is a time ordering operator. We also diagonalize the final Hamiltonian $H(t_f) = \sum_m (E_m g_m^\dagger g_m - E_m g_m g_m^\dagger)$, with $E_m < 0$. The number of excitations then is

$$n_{\rm ex} = \sum_m \langle\psi_f|g_m g_m^\dagger|\psi_f\rangle. \quad (8)$$

Figures 2(c)–2(d) illustrate the number of excitations for the two quench processes. Clearly, the KZM excitations will be more effectively suppressed for longer quench times t_Q. In particular, process I gives rise to no excitations, whereas process II yields excitations with universal number 1 agreeing with our previous analysis.

More generally, excitations in the spin model can exhibit complex spin configurations, which can be difficult to detect exactly in experiments. To exhibit the excitations in the spin ladder unambiguously, one can drive the system into the Ising limit ($J_n^z \gg J^x, J^y$). In this limit, the ground state exhibits a parallel alignment of each pair of rung spins from two chains ($\langle\sigma_{2n-1}^z\sigma_{2n}^z\rangle = 1$), whereas the lowest excitation corresponds to an antiparallel alignment of a single pair of rung spins ($\langle\sigma_{2n-1}^z\sigma_{2n}^z\rangle = -1$). This excitation can in practice be measured in experiments. Therefore, a MF qubit state clearly can be experimentally read out through measurement of the excitations emerging in the quenched inhomogeneous spin ladder.

Non-Abelian braiding statistics. First, we design a spin ladder model with T-junction structure to implement the braiding operation of MFs. Our model is composed of three ladders joining to form a hexagon, as depicted in Fig. 3(a).

A similar T-junction design for braiding MFs in spin ladders has been proposed earlier.[37] However, their T-junction model cannot be solved exactly, which obscures the fate of the non-Abelian braiding statistics in their MF model. In contrast, one notes that with our special design of three ladders and a hexagon-junction structure, each site always has three different links. Therefore, this model can be solved exactly using the Majorana fermionization technique with all the u_{ij} commuting with the Hamiltonian. Following the same procedures as before, we obtain a fermionic Hamiltonian $H = \sum_{\alpha=a,b,c} H_\alpha + H_t$, with

$$H_\alpha = \sum_{n=1}^{N-1}[(\omega_{\alpha,n} f_{\alpha,n}^\dagger f_{\alpha,n+1} + \Delta_{\alpha,n} f_{\alpha,n} f_{\alpha,n+1} + \text{H.c.}) + \mu_{\alpha,n}(2f_{\alpha,n}^\dagger f_{\alpha,n} - 1)] \quad (9)$$

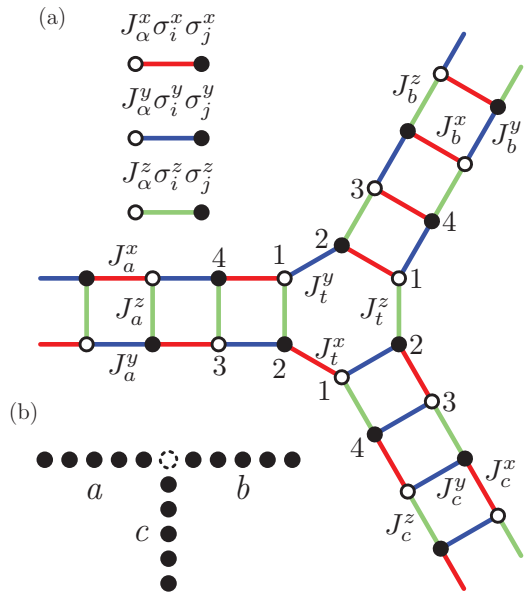

FIG. 3. (Color online) (a) Trijunction spin ladders. Three spin ladders (a,b,c) joining to form a hexagon (t). (b) The effective T junction of Kitaev's SC wire. Compared with the model in Ref. 3, the central site at the T junction (white dotted site) is missing in our model.

and

$$H_t = \sum A_{\alpha\beta}(f_{\alpha,1}^\dagger f_{\beta,1} + f_{\alpha,1} f_{\beta,1} + \text{H.c.}), \quad (10)$$

where $\mu_{a(b,c),n} = 2J^{z(x,y)}_{a(b,c),n} u^{a(b,c)}_{2n+1,2n+2}$, $A_{ab(bc,ca)} = J_t^{y(z,x)} u_{ab(bc,ca)}$, and $\Delta_{a(b,c),n}(\omega_{a(b,c),n}) = J^{x(y,z)}_{a(b,c),n} u^{a(b,c)}_{2n+1,2n+4} \pm J^{y(z,x)}_{a(b,c),n} u^{a(b,c)}_{2n+2,2n+3}$. Similarly to the previous case, with $J^{x(y,z)}_{a(b,c),n}$, $J^{y(z,x)}_{a(b,c),n}$, and $J_t^{y(z,x)}$ positive, the ground state corresponds to all $u_{ij} = 1$.

The T-junction spin ladder has been mapped into the p wave of Kitaev's SC wire with a T-junction structure, as shown in Fig. 3(b). This effective T-junction Kitaev wire differs slightly from the model in Ref. 3. In particular, the phase of the pairing term in our spin model cannot take complex values; its phase can only be 0 or π, the change being achieved by adjusting the relative value of intrachain coupling $J^{x(y,z)}_{a(b,c)}, J^{y(z,x)}_{a(b,c)}$. To realize braiding for MFs, it is important that no additional MFs appear at the T junction. Therefore, the phase of the pairing term should be different for the wire pairs (a,c) and (b,c).[3] We can choose the pairing phase of wire a and b is chosen to be 0, whereas that of wire c is chosen to be π. To achieve this, we can simply put $J_a^x > J_a^y$, $J_b^y > J_b^z$, and $J_c^z < J_c^x$.

To verify unambiguously the braiding statistics, we performed numerical simulations on the nonequilibrium processes that have the MFs braiding counterclockwise, as illustrated in Fig. 4(a), I–III. After braiding a finite (1–4) times, we performed the qubit readout procedure by driving the whole system nontopologically and then measuring the emergent fusion excitations, as shown in Fig. 4(a), IV. We begin with four MFs (γ_1,γ_2) and (γ_3,γ_4), whose state can be written as $|00\rangle$ in the basis of $f_A = \gamma_1 + i\gamma_2$ and $f_B = \gamma_3 + i\gamma_4$; our measurement scheme reads off the qubit state in this basis.

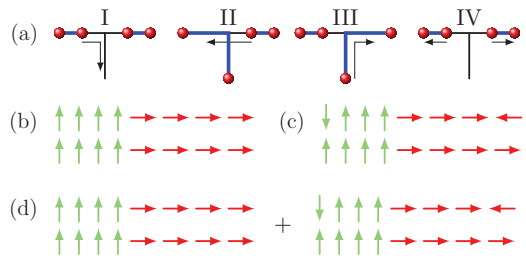

FIG. 4. (Color online) (a) Steps for braiding and reading off the MFs qubit states. Schematic representation for the quantum state in the large interchain coupling limit; here we omit the ladder c for simplicity. (b) Ground state of the system: spins on the ladder a (b) align parallel along the z (x) direction. (c) Output state by braiding MFs twice: excited state with two excitations located at the left and right ends. (d) Output state by braiding MFs one (three) times: equally weighted superposition of two states (b) and (c).

The braiding of MFs γ_2 and γ_3 can be described by the unitary operator $U = \exp(\pi\gamma_2\gamma_3/4)$. If MFs braid one or three times, the qubit state is $(|00\rangle \pm |11\rangle)/\sqrt{2}$; if MFs braid twice, the qubit state is $|11\rangle$. Furthermore, the qubit state changes back into the initial state $|00\rangle$ if the MFs braid four times. Our numerical calculations confirm those results.[41] In particular, we have found the emergence of one or two excitations after the process with MFs braiding one (three) or two times, with each half of the excitations emerging at the left (right) end of the a (b) ladder. Finally, braiding MFs four times produces no excitations.

The general scheme to illustrate the non-Abelian braiding statistics can be visualized as follows. First we prepare a nontopological state, schematically shown in Fig. 4(b). To create and manipulate the MFs, one needs simply to change the interchain coupling strengths of three ladders. After braiding the MFs one or three times and driving the system back into a nontopological phase, one obtains a quantum state as shown in Fig. 4(d). After braiding the MFs twice, one obtains two excitations localized at the ends of spin ladders a and b, as shown in Fig. 4(c). Finally, if one performs the braiding of the MFs four times, the system returns to its ground state.

Summary. We have proposed and numerically shown that, in a quenched inhomogeneous spin ladder model, one can read out the MF qubit state by measuring the MF fusion excitations. An exactly solvable T-junction spin ladder model is shown to implement MF braiding operations. With numerical simulation of nonequilibrium braiding, we show that the MF in our model obeys non-Abelian braiding statistics. Our proposal could be realized and tested in future experimental systems of ultracold atoms or SC circuits.

Acknowledgments. We acknowledge J. Q. You, Y. Yu, and P. Hohenberg for useful discussions. Y.-C.H. appreciates the help of Y.-Y. Zhao, K. Ding, and J.-D. Zang. This work was supported by the State Key Programs of China (Grants No. 2012CB921604 and No. 2009CB929204), the National Natural Science Foundation of China (Grants No. 11074043 and No. 11274069), and Shanghai Municipal Government, the GRF grant (Grant No. HKU7058/11P) of the RGC of Hong Kong.

[1] E. Majorana, Nuovo Cimento **14**, 171 (1937).
[2] D. A. Ivanov, Phys. Rev. Lett. **86**, 268 (2001).
[3] J. Alicea, Y. Oreg, G. Refael, F. von Oppen, and M. P. A. Fisher, Nat. Phys. **7**, 412 (2011).
[4] C. Nayak, S. H. Simon, A. Stern, M. Freedman, and S. Das Saram, Rev. Mod. Phys. **80**, 1083 (2008).
[5] G. Moore and N. Read, Nucl. Phys. B **360**, 362 (1991).
[6] N. Read and D. Green, Phys. Rev. B **61**, 10267 (2000).
[7] A. Stern and B. I. Halperin, Phys. Rev. Lett. **96**, 016802 (2006).
[8] P. Bonderson, A. Kitaev, and K. Shtengel, Phys. Rev. Lett. **96**, 016803 (2006).
[9] L. Fu and C. L. Kane, Phys. Rev. Lett. **100**, 096407 (2008).
[10] M. Sato, Y. Takahashi, and S. Fujimoto, Phys. Rev. Lett. **103**, 020401 (2009).
[11] A. Y. Kitaev, Phys. Usp. **44**, 131 (2001).
[12] S. Tewari, S. Das Saram, C. Nayak, C. Zhang, and P. Zoller, Phys. Rev. Lett. **98**, 010506 (2007).
[13] F. Hassler, A. R. Akhmerov, C.-Y. Hou, and C. W. J. Beenakker, New. J. Phys. **12**, 125002 (2010).
[14] C. J. Bolech and E. Demler, Phys. Rev. Lett. **98**, 237002 (2007).
[15] S. Tewari, C. Zhang, S. Das Saram, C. Nayak, and D.-H. Lee, Phys. Rev. Lett. **100**, 027001 (2008).
[16] A. R. Akhmerov, J. Nilsson, and C. W. J. Beenakker, Phys. Rev. Lett. **102**, 216404 (2009).
[17] Y. Tanaka, T. Yokoyama, and N. Nagaosa, Phys. Rev. Lett. **103**, 107002 (2009).
[18] K. T. Law, P. A. Lee, and T. K. Ng, Phys. Rev. Lett. **103**, 237001 (2009).
[19] K. Flensberg, Phys. Rev. Lett. **106**, 090503 (2011).
[20] S.-L. Zhu, L.-B. Shao, Z. D. Wang, and L.-M. Duan, Phys. Rev. Lett. **106**, 100404 (2011).
[21] L. Jiang, D. Pekker, J. Alicea, G. Refael, Y. Oreg, and F. von Oppen, Phys. Rev. Lett. **107**, 236401 (2011).
[22] J. D. Sau, R. M. Lutchyn, S. Tewari, and S. Das Sarma, Phys. Rev. Lett. **104**, 040502 (2010); J. Alicea, Phys. Rev. B **81**, 125318 (2010); R. M. Lutchyn, J. D. Sau, and S. Das Saram, Phys. Rev. Lett. **105**, 077001 (2010); Y. Oreg, G. Refael, and F. von Oppen, *ibid*. **105**, 177002 (2010).
[23] V. Mourik, K. Zuo, S. M. Frolov, S. R. Plissard, E. P. A. M. Bakkers, and L. P. Kouwenhoven, Science **336**, 1003 (2012); A. Das, Y. Ronen, Y. Most, Y. Oreg, M. Heiblum, and H. Shtrikman, Nat. Phys. **8**, 887 (2012); M. T. Deng, C. L. Yu, G. Y. Huang, M. Larsson, P. Caroff, and H. Q. Xu, Nano Lett. **12**, 6414 (2012).
[24] L. P. Rokhinson, X. Liu, and J. K. Furdyna, Nat. Phys. **8**, 795 (2012); J. R. Williams, A. J. Bestwick, P. Gallagher, S. S. Hong, Y. Cui, A. S. Bleich, J. G. Analytis, I. R. Fisher, and D. Goldhaber-Gordon, Phys. Rev. Lett. **109**, 056803 (2012).
[25] J. Liu, A. C. Potter, K. T. Law, and P. A. Lee, Phys. Rev. Lett. **109**, 267002 (2012).
[26] J. D. Sau, E. Berg, and B. I. Halperin, arXiv:1206.4596.
[27] A. Kitaev, Ann. Phys. (NY) **321**, 2 (2006).
[28] L.-M. Duan, E. Demler, and M. D. Lukin, Phys. Rev. Lett. **91**, 090402 (2003).
[29] H. Weimer, M. Müller, I. Lesanovsky, P. Zoller, and H. P. Büchler, Nat. Phys. **6**, 382 (2010).

[30] J. Q. You, X.-F. Shi, X. Hu, and F. Nori, Phys. Rev. B **81**, 014505 (2010).

[31] R. Schmied, J. H. Wesenberg, and D. Leibfried, New J. Phys. **13**, 115011 (2011).

[32] S. R. Manmana, E. M. Stoudenmire, K. R. A. Hazzard, A. M. Rey, and A. V. Gorshkov, Phys. Rev. B **87**, 081106(R) (2013); A. V. Gorshkov, K. R. A. Hazzard, and A. M. Rey, Mol. Phys. **111**, 1908 (2013).

[33] Z.-L. Xiang, S. Ashhab, J. Q. You, and F. Nori, Rev. Mod. Phys. **85**, 623 (2013).

[34] A. Saket, S. R. Hassan, and R. Shankar, Phys. Rev. B **82**, 174409 (2010).

[35] Y. Tserkovnyak and D. Loss, Phys. Rev. A **84**, 032333 (2011).

[36] W. DeGottardi, D. Sen, and S. Vishveshwara, New J. Phys. **13**, 065028 (2011).

[37] F. L. Pedrocchi, S. Chesi, S. Gangadharaiah, and D. Loss, Phys. Rev. B **86**, 205412 (2012).

[38] T. W. B. Kibble, J. Phys. A **9**, 1387 (1976); W. H. Zurek, Nature (London) **317**, 505 (1985).

[39] J. Dziarmaga, Adv. Phys. **59**, 1063 (2010); A. Polkovnikov, K. Sengupta, A. Silva, and M. Vengalattore, Rev. Mod. Phys. **83**, 863 (2011).

[40] J. Dziarmaga, P. Laguna, and W. H. Zurek, Phys. Rev. Lett. **82**, 4749 (1999); J. Dziarmaga and M. M. Rams, New J. Phys. **12**, 055007 (2010); A. del Campo, G. De Chiara, G. Morigi, M. B. Plenio, and A. Retzker, Phys. Rev. Lett. **105**, 075701 (2010).

[41] See Supplemental Material at http://link.aps.org/supplemental/10.1103/PhysRevB.88.180402 for mathematical details of numerical calculations, energy spectra during the two processes, as well as numerical results of MFs braiding.